Bioorganic & Medicinal Chemistry 19 (2011) 1085–1096

Contents lists available at ScienceDirect

Bioorganic & Medicinal Chemistry

journal homepage: www.elsevier.com/locate/bmc

In vivo MR/optical imaging for gastrin releasing peptide receptor of prostate cancer tumor using Gd-TTDA-NP-BN-Cy5.5

Ying-Hsiu Lin [a,†], Kasala Dayananda [a,†], Chiao-Yun Chen [b,c], Gin-Chung Liu [b,c], Tsai-Yueh Luo [d], Hui-Sheng Hsu [e], Yun-Ming Wang [a,*]

[a] Department of Biological Science and Technology, National Chiao Tung University, 75 Bo-Ai Street, Hsinchu 300, Taiwan
[b] Department of Medical Imaging, Kaohsiung Medical University Hospital, Kaohsiung Medical University, 100 Shih-Chuan 1st Road, Kaohsiung 807, Taiwan
[c] Department of Radiology, Kaohsiung Medical University, 100 Shih-Chuan 1st Road, Kaohsiung 807, Taiwan
[d] Isotope Application Division, Institute of Nuclear Energy Research, 1000 Wenhua Road, longtan, Taoyuan County 325, Taiwan
[e] Graduate Institute of Medicine College of Medicine and Department of Medical Imaging, Kaohsiung Municipal Hsiao-Kang Hospital, Kaohsiung Medical University, 100 Shih-Chuan 1st Road, Kaohsiung 807, Taiwan

ARTICLE INFO

Article history:
Received 25 February 2010
Revised 13 April 2010
Accepted 15 April 2010
Available online 21 April 2010

Keywords:
Magnetic resonance imaging
Gastrin releasing peptide (GRP) receptor
Bombesin
Peptide
Fluorescence

ABSTRACT

Magnetic resonance imaging (MRI) has become the leading imaging tool for providing fine anatomical and physiology details. Optical imaging is offering a sensitive and specific method for in vivo molecular imaging of targeting molecules. The goal of this study is to design, synthesize, and characterize a new target-specific dual contrast agent for MR and optical imaging. Hence, $[Gd(TTDA\text{-}NP)(H_2O)]^{2-}$ was prepared and characterized. In addition, an 8-amino acid Bombesin analogue (BN) peptide substrate, which can target prostate, breast, and colon cancer, was synthesized by solid-phase peptide synthesis and subsequently conjugated with $[Gd(TTDA\text{-}NP)(H_2O)]^{2-}$ to form BN conjugated Gd-TTDA-NP-BN. The water-exchange rate (k_{ex}^{298}) for $[Gd(TTDA\text{-}NP)(H_2O)]^{2-}$ ($110 \times 10^6\ s^{-1}$) is significantly higher than that of $[Gd(DTPA)(H_2O)]^{2-}$ complex and the rotational correlation time (τ_R) for $[Gd(TTDA\text{-}NP)(H_2O)]^{2-}$ (145 ps) is also higher than those of $[Gd(TTDA)(H_2O)]^{2-}$ (104 ps) and $[Gd(DTPA)(H_2O)]^{2-}$ (103 ps). The Gd-TTDA-NP-BN shows remarkable high relaxivity ($7.12\ mM^{-1}\ s^{-1}$) comparing to that of $[Gd(TTDA\text{-}NP)(H_2O)]^{2-}$. The fluorescence studies showed that the Gd-TTDA-NP-BN could efficiently enter PC-3 cells. Additionally, the human cancer cells xenografts using Gd-TTDA-NP-BN-Cy5.5 as an optical imaging probe clearly visualized subcutaneous PC-3 tumor and demonstrated its targeting ability to the gastrin releasing peptide (GRP) receptor overexpression. Furthermore, the biodistribution studies demonstrated significantly high tumor uptake (25.97 ± 1.07% ID/g) and high tumor-to-normal tissue ratios at one hour post-injection of Gd-TTDA-NP-BN-Cy5.5 in the animal model. These results suggest that the Gd-TTDA-NP-BN-Cy5.5 is a superior probe for in vivo optical imaging. Importantly, the MR imaging studies showed notable signal enhancement (44.9 ± 4.2%) on the tumor, indicating a high level accumulation of the contrast agent within the PC-3 tumor sites. Hence, targeting of prostate cancer cells was observed under in vitro and in vivo MR imaging studies using Gd-TTDA-NP-BN contrast agent. We conclude that Gd-TTDA-NP-BN and Gd-TTDA-NP-BN-Cy5.5 can be potentially used as the contrast agents for targeting GRP receptor overexpressing cells and tumors.

1. Introduction

Molecular imaging is providing a sensitive and specific method for the detection and localization of the biochemical appearance in vivo.[1] Recently, some progress in tumor-targeted imaging by positron emission tomography (PET)[2–4] has been made with the assist of Bombesin complexes labeled with radioactive isotopes.[5–8] However, radionuclide imaging may suffer from low photon counts requiring long scan times as well as from a finite half-life and radiation dosage preventing longitudinal imaging in patients.[9] Magnetic resonance imaging (MRI) offers several advantages over other clinical diagnostic techniques in molecular imaging, including high spatial resolution, noninvasiveness, high anatomical contrast, and lack of harmful radiation.[10–12] On the other hand, sensitivity of MRI in depicting a small molecule is constrained by the ubiquitous protons in the body, resulting in a high background and low signal to noise ratio (SNR). Hence, the alternative amplification strategies using smart contrast agents are required. In addition, noninvasive imaging protease activity is very important for personalized diagnosis and therapy in treating diseases.[9,13]

* Corresponding author. Tel.: +886 3 5721212x56972; fax: +886 3 5729288.
E-mail address: ymwang@mail.nctu.edu.tw (Y.-M. Wang).
† These two authors contributed equally.

0968-0896/$ - see front matter © 2010 Elsevier Ltd. All rights reserved.
doi:10.1016/j.bmc.2010.04.040

Over the past few years, optical imaging techniques have been established as powerful tools for in vivo molecular imaging of specific target structures. Although poor light penetration through tissues makes their utilization in human difficult, these techniques have been effectively used in preclinical small animal research.[14,15] Near-infrared (NIR) fluorescence imaging, which uses neither ionizing radiation nor radioactive materials, is emerging as a complement to nuclear imaging methods. The cyanine dye 5.5 (Cy5.5), a NIR fluorescent dye has proven to be a promising in vivo probe. It has an absorbance maximum at 675 nm and emission maximum at 694 nm and can be detected in vivo at subnanomolar quantities and at depths sufficient for experimental and clinical imaging.[16,17]

Bombesin (BN) is a small peptide containing 14 amino acids (Glu-Gln-Arg-Leu-Gly-Asn-Gln-Trp-Ala-Val-Gly-His-Leu-Met-NH_2). It was originally isolated from the skin of amphibian *Bombina orientalis*.[18,19] The BN-like peptides have very high binding affinity for the gastrin releasing peptide (GRP) receptor and produce a wide range of biological responses in peripheral tissues as well as in the central nervous system, including stimulation of gastrointestinal hormone release, exocrine secretion, and maintenance of circadian rhythms.[20,21] In addition, it has been documented that the BN peptides promote proliferation in cancer cells.[22] The overexpression of GRP receptor has been demonstrated in a large number of tumors, including prostate, breast, colon, and small cell lung cancer.[23–25] In the past few years, the highly GRP receptor overexpressing tumor is emerging as an attractive target for both cancer therapy and early detection and Bombesin or its analogues labeled with different radionuclides had been widely used for tumor imaging.[26,27]

Thermodynamically stable, water-soluble, and highly paramagnetic Gd(III) complexes, each bearing a multidentate ligand and at least one coordinated water molecule, have demonstrated high relaxivity and have therefore been served as versatile MR imaging contrast agents. Recently, our group and other research groups have developed asymmetry poly(aminocarboxylates) derivatives of 3,6,10-tri(carboxymethyl)-3,6,10-triazadodecanedioic acid (TTDA) and their Gd(III) complexes have shown to possess fast water-exchange rates.[28–32] Although, the water-residence lifetime has a minor influence on relaxivity of small molecular contrast agents but it has a significant influence on relaxivity of macromolecular contrast agents.[33,34] The ligand TTDA was chosen because the water-residence lifetimes for $[Gd(TTDA)(H_2O)]^{2-}$ and its derivatives are significantly lower than that of $[Gd(DTPA)(H_2O)]^{2-}$ (DTPA = 3,6,9-tri(carboxymethyl)-3,6,9-triazaundecanedioic acid) and has reached the optimal value. Recently, Bombesin conjugated $[Gd(DOTA)(H_2O)]^{-}$ derivative as a MRI contrast agent.[35] However, the detailed MR imaging study has not yet reported. In this regard, we synthesized and characterized a new contrast agent for optical and MR imaging studies. The (*N*-(1-methylene(*p*-isohiocyanatophenol)di(carboxymethyl) triazadodecanedioic acid (TTDA-NP) was conjugated with Bombesin analogue (Lys-Gly-Gly-Gly-Gln-Trp-Ala-Val-Gly-His-Leu-Met-NH_2) peptide (TTDA-NP-BN), BN conjugated to target GRP receptor expressing tumor cells. The synthetic strategy of Gd-TTDA-NP-BN was depicted in Scheme 1. Subsequently, cyanine dye was conjugated to Gd-TTDA-NP-BN complex for optical imaging studies. We also evaluated the cell cytotoxicity of Gd-TTDA-NP-BN to PC-3 cells which is a human prostate cancer cell line with overexpressing gastrin releasing peptide (GRP) receptors and KB cells, human nasopharyngeal epidermal carcinoma cell line, lacking of the expression of GRP receptors. In addition, in vitro assays were tested using PC-3 cells to evaluate the cellular uptake and cellular retention. In vitro and in vivo optical imagings were studied to demonstrate the targeting ability toward GRP receptor overexpression cells and tumors. Furthermore, in vitro and in vivo T_1-weighted MR imaging studies of cells and tumor-bearing mice were also investigated.

2. Results and discussion

2.1. Synthesis of Gd-TTDA-NP-BN and Gd-TTDA-NP-BN-Cy5.5

In this study, we reported the Gd-TTDA-NP-BN and Gd-TTDA-NP-BN-Cy5.5 complexes for molecular MR imaging and optical imaging. Scheme 1 shows the schematic representation of the synthesis of Gd-TTDA-NP-BN, Gd-TTDA-NP-BN-Cy5.5, and Eu-TTDA-NP-BN. The ligand TTDA-NP-BN was synthesized in four steps. In the first step, 3,6,10-triazadodecane-3,10-tetraacetic acid (tetra)-*tert*-butyl ester (TTDA-4est) was treated with 2-hydroxy-5-nitrobenzyl bromide in the presence of anhydrous K_2CO_3 in CH_3CN at 80 °C for 20 h under nitrogen atmosphere. The resulting product (TTDA-NP) was purified by silica gel column chromatography. Subsequently, the hydrogenation was performed in the presence of Pd/C catalyst in methanol at room temperature. The product (TTDA-NP-NH_2) was purified by column chromatography. In the next step, it was required to convert the aromatic amine to a more reactive isothiocyanate functional group for peptide conjugation. TTDA-NP-NH_2 was treated with thiophosgene in THF at 60 °C for overnight. The crude product (TTDA-NP-NCS) was purified by column chromatography. Finally, the Bombesin analogue (BN) (Lys-Gly-Gly-Gly-Gln-Trp-Ala-Val-Gly-His-Leu-Met-NH_2) peptide was conjugated with TTDA-NP-NCS ligand, to obtain TTDA-NP-BN after preparative HPLC purification. The ESI mass spectrum shown in Figure S1 (see Supplementary data) confirms its identity. The Gd-TTDA-NP-BN complex was obtained by complexation of Gd(III) ion with TTDA-NP-BN ligand in water at room temperature for 18 h. The resulting complex was identified by MS (ESI), as shown in Figure S2. The Gd-TTDA-NP-BN-Cy5.5 was achieved through conjugation of NHS-Cy5.5 ester with amino group of lysine residue of the Gd-TTDA-NP-BN, purified by preparative HPLC, and identified by MS (ESI).

2.2. ^{17}O NMR study

Kinetic parameters were determined for $[Gd(TTDA\text{-}NP)(H_2O)]^{2-}$ by variable-temperature ^{17}O NMR studies. The chemical shifts ($\Delta\omega_r$), the longitudinal ($1/T_{1r}$), and transverse ($1/T_{2r}$) relaxation rates were analyzed simultaneously (using Eqs. 1S–9S in the Supplementary data). The data for $[Gd(TTDA\text{-}NP)(H_2O)]^{2-}$ are plotted in Figure S3 and the corresponding curves represent the results of the best fitting of the data according to Eqs. (1S–9S). As shown in the Table S1, the large number of parameters is influencing the data obtained by the different techniques. However, the ^{17}O NMR technique has an advantage that the outer-sphere contributions to the relaxation rates are negligibly small, which is a result of the oxygen nucleus being closer to the paramagnetic center when it is bound in the inner sphere. The scalar coupling constant ($A/\hbar$) of $[Gd(TTDA\text{-}NP)(H_2O)]^{2-}$ is very similar to those which are obtained for other Gd(III) complexes (-3.2 ± 0.3 and $-3.8 \pm 0.2 \times 10^6$ rad s^{-1} for $[Gd(TTDA)(H_2O)]^{2-}$ and $[Gd(DTPA)(H_2O)]^{2-}$, respectively) with one inner-sphere water molecule. In the overall temperature range, the transverse ^{17}O relaxation rates ($1/T_{2r}$) decrease with an increasing temperature, indicating that this system is in the fast exchange regime.[36] Hence, $1/T_{2r}$ is determined by the relaxation rate of the coordinated water molecule ($1/T_{2m}$), which is influenced by the water-residence lifetime ($\tau_M = 1/k_{ex}$), the longitudinal electronic relaxation rate ($1/T_{1e}$), and the scalar coupling constant ($A/\hbar$). The k_{ex}^{298} ($110 \pm 13 \times 10^6$ s^{-1}) value of $[Gd(TTDA\text{-}NP)(H_2O)]^{2-}$ is similar to those of other $[Gd(TTDA)(H_2O)]^{2-}$ derivatives, which is significantly higher than that of $[Gd(DTPA)(H_2O)]^{2-}$ ($k_{ex}^{298} = 4.1 \pm 0.3 \times 10^6 s^{-1}$). Moreover, the value of correlation time (τ_R) for Gd(III) complex with TTDA-NP was obtained at 298 K from the fitting of ^{17}O NMR. The τ_R

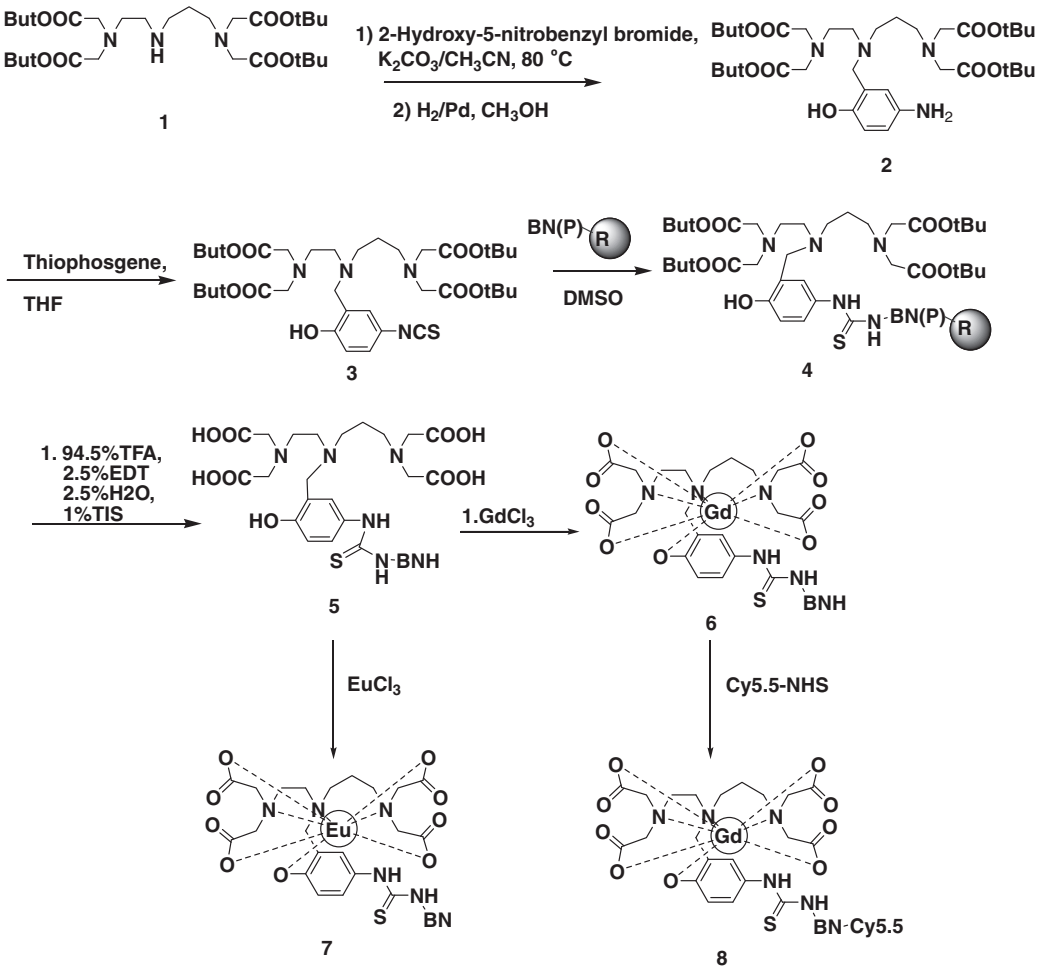

Scheme 1. Synthetic scheme of Gd-TTDA-NP-BN, Gd-TTDA-NP-BN-Cy5.5, and Eu-TTDA-NP-BN.

value of $[Gd(TTDA\text{-}NP)(H_2O)]^{2-}$ (145 ps) is higher than those of $[Gd(TTDA)(H_2O)]^{2-}$ (104 ps)[37] and $[Gd(DTPA)(H_2O)]^{2-}$ (103 ps).[38]

2.3. Luminescence study

To determine the number of inner sphere water by luminescence method,[39–41] the $[Eu(TTDA\text{-}NP)(H_2O)]^{2-}$ complex was synthesized. The luminescence lifetime (τ) has been measured in both water and deuterium oxide upon excitation at 395 nm. The $[Eu(TTDA\text{-}NP)(H_2O)]^{2-}$ complex contains 0.92 and 0.72 inner-sphere water molecules calculated by using (Eqs. 1 and 2) as follows

$$q = 1.05[1/\tau_{H_2O} - 1/\tau_{D_2O}] \quad (1)$$

$$q = ([1/\tau_{H_2O} - 1/\tau_{D_2O}] - 0.25) \times 1.2 \quad (2)$$

where q is the number of water molecules bound to metal ions, τ_{H2O} luminescence half-life in water solution and τ_{D2O} is the luminescence half-life in deuterium oxide solution, respectively. The q value is obtained from the luminescence study.

2.4. Relaxivity

In order to obtain the relaxivity of Gd(III) complex, we measured the proton spin-lattice relaxation time for $[Gd(TTDA\text{-}NP)(H_2O)]^{2-}$ and Gd-TTDA-NP-BN complexes at 37.0 ± 0.1 °C and 20 MHz. The relaxivity (r_1) values were shown in Table 1. The Gd-TTDA-NP-BN exhibits substantially higher longitudinal relaxivity than that of $[Gd(TTDA\text{-}NP)(H_2O)]^{2-}$, because $[Gd(TTDA\text{-}NP)(H_2O)]^{2-}$ conjugated with BN peptide reduces the tumbling rate and enhances its relaxivity. It is known that $[Gd(TTDA\text{-}NP)(H_2O)]^{2-}$ has one inner-sphere water molecule and exhibits higher water-exchange rate than those of $[Gd(DTPA)(H_2O)]^{2-}$ derivatives.[42] Significantly, the relaxivity of $[Gd(TTDA\text{-}NP)(H_2O)]^{2-}$ complex is slightly higher than those of $[Gd(TTDA)(H_2O)]^{2-}$ and $[Gd(DTPA)\text{-}(H_2O)]^{2-}$.

Table 1
Relaxivity (r_1) of $[Gd(TTDA\text{-}NP)(H_2O)]^{2-}$, [Gd-TTDA-NP-BN] $[Gd(TTDA)(H_2O)]^{2-}$, and $[Gd(DTPA)(H_2O)]^{2-}$, at 37.0 ± 0.1 °C and 20 MHz

Complex	pH	Relaxivity r_1/mM^{-1}s^{-1}
$[Gd(TTDA\text{-}NP)(H_2O)]^{2-}$	7.4 ± 0.1	4.16 ± 0.08
[Gd-TTDA-NP-BN]	7.4 ± 0.1	7.12 ± 0.05
$[Gd(TTDA)(H_2O)]^{2-}$ [a]	7.5 ± 0.1	3.85 ± 0.03
$[Gd(DTPA)(H_2O)]^{2-}$ [b]	7.6 ± 0.1	3.89 ± 0.03

[a] Data was obtained from Ref. 37.
[b] Ref. 42.

2.5. Cell cytotoxicity

In vitro cell cytotoxicity is an important parameter for Gd-TTDA-NP-BN complex to apply to molecular imaging. In this study, the MTT assay was performed to evaluate cytotoxicity of Gd(III) complex against PC-3 and KB cells. The various concentrations of Gd(III) complex were incubated with PC-3 and KB cell lines, after 24 h the cell viability was examined. Figure 1 showed that more than

90% cell viability was observed after 24 h of incubation under high concentration of Gd-TTDA-NP-BN complex. These results indicated that the Gd-TTDA-NP-BN exhibited low cytotoxicity.

2.6. In vitro optical imaging

In this study, Eu-TTDA-NP-BN was used to evaluate the specificity of Gd-TTDA-NP-BN to PC-3 cells using fluorescence microscopy. The Eu-TTDA-NP-BN complex was incubated with PC-3 cells at 4.0 and 37.0 °C. The specific tumor cell uptake of the Bombesin analogue conjugated complex (Eu-TTDA-NP-BN) was visualized under fluorescence microscopy. Figure 2A–C showed that the fluorescence image of PC-3 cells incubated with or without of Eu-TTDA-NP-BN, at 4.0 and 37.0 °C, respectively. These results indicated that the PC-3 cells had produced strong fluorescence intensity at 37.0 °C. In contrast, the PC-3 cells have shown weak fluorescence at 4.0 °C, because the complex only binds to cell membrane and cannot enter into cells at low temperature. Hence, the cellular uptake of Eu-TTDA-NP-BN was high at the physiological temperature, comparing to at low temperature.

Additionally, we synthesized the near-infrared dye conjugated with Gd(III) complex (Gd-TTDA-NP-BN-Cy5.5) and carried out an in vitro study to demonstrate the targeting of probe to GRP receptor. In order to assess the binding specificity of Gd-TTDA-NP-BN-Cy5.5 to GRP receptor, the complex was incubated with PC-3 and KB cells. The fluorescence images were studied, as shown in Figure 3A and B. Figure 3A shows the red fluorescence originated from targeting of probe to PC-3 cells and the cell image with nucleus stained with blue DAPI dye was overlay with Cy5.5 fluorescence image. The resulted fluorescence images clearly demonstrate that the Gd(III) complex interacts only with cells, but not with nucleus. In addition, the PC-3 cells had displayed strong fluorescence. These data confirmed that the Gd-TTDA-NP-BN-Cy5.5 complex could be specifically target to PC-3 cells. In contrast, KB cells did not exhibit red fluorescence as shown in Figure 3B because of no GRP receptor overexpression. These results imply that Gd-TTDA-NP-BN-Cy5.5 could efficiently bind to GRP receptor.

2.7. In vivo optical imaging

The in vivo optical imaging studies were performed in PC-3 tumor, which is GRP receptor overexpressed. The solution of Gd-TTDA-NP-BN-Cy5.5 complex (10 nmol) was injected to nude mice bearing PC-3 and KB tumors through tail vein. Figure 4A–C illustrated in vivo optical images of mice at 0.5 h after injection of Gd-TTDA-NP-BN-Cy5.5 by white light, NIR fluorescence, and color mapping, respectively. The NIR imaging demonstrates the

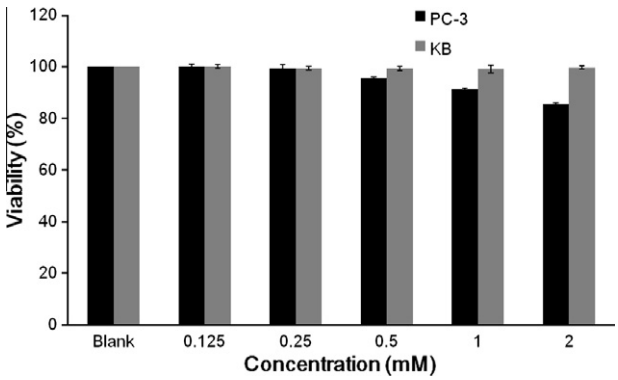

Figure 1. Cytotoxicity of Gd-TTDA-NP-BN incubated with KB cells (black) and PC-3 cells (gray) for 24 h. Concentration dependence (100–1000 μM) of MTT assay graph observed in vitro cell viability after incubating of Gd-TTDA-NP-BN.

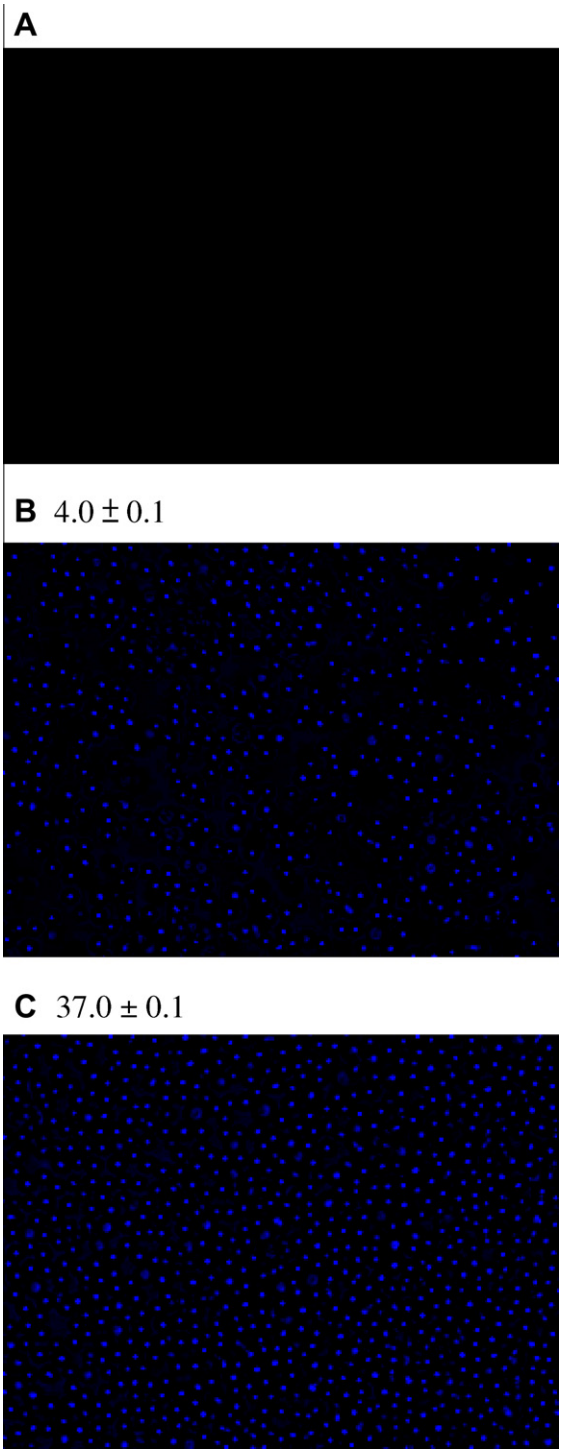

Figure 2. Fluorescence microscope imaging (A) PC-3 Cells incubated without Eu-TTDA-NP-BN, (B) PC-3 cells incubated with Eu-TTDA-NP-BN at 4.0 °C, and (C) PC-3 cells incubated with Eu-TTDA-NP-BN at 37.0 °C.

uptake of Gd-TTDA-NP-BN-Cy5.5 in the region of the tumor. As shown in Figure 4B, a strong fluorescence enhancement was observed for PC-3 tumor cells. In contrast, no obvious fluorescence enhancement was found for negative KB tumor owing to lack of GRP receptor expression. These results indicate that the Gd-TTDA-NP-BN-Cy5.5 has the ability to target PC-3 tumor in vivo. Furthermore, optical imaging was conducted at predetermined time intervals from 0.5 to 24.0 h after injection, as shown in Figure 5A and B. The subcutaneous PC-3 tumor could be clearly visualized

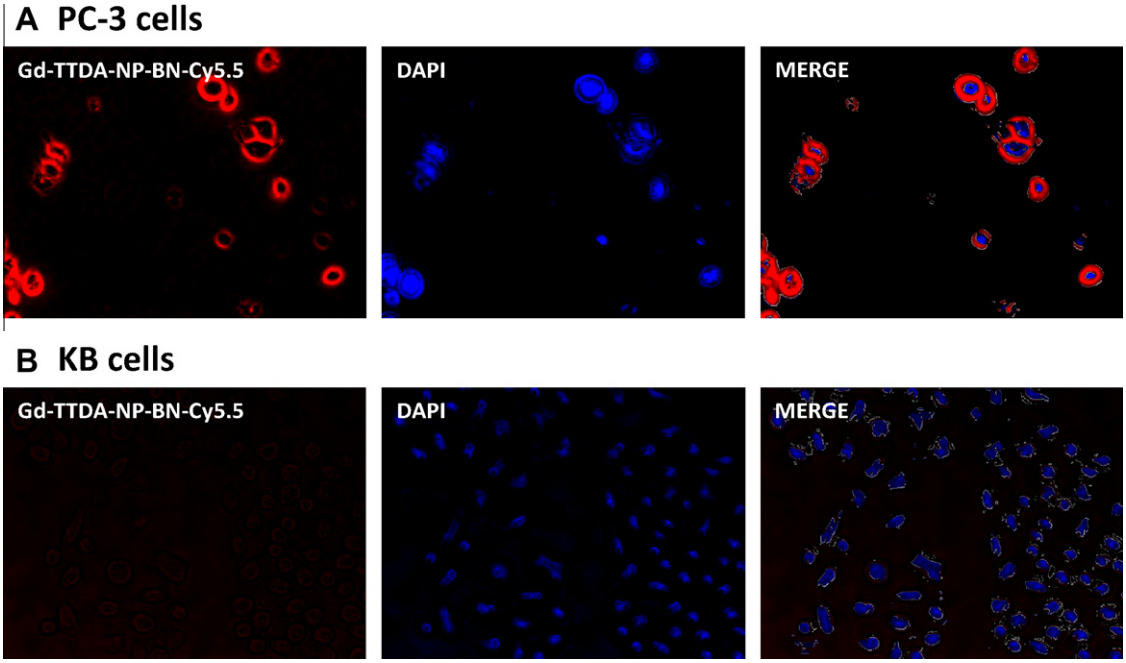

Figure 3. Fluorescence microscopy assays of Gd-TTDA-NP-BN-Cy5.5 binding to GRP receptor. The signals of Gd-TTDA-NP-BN-Cy5.5 (10 μM) and DAPI are displayed in red and blue, respectively.

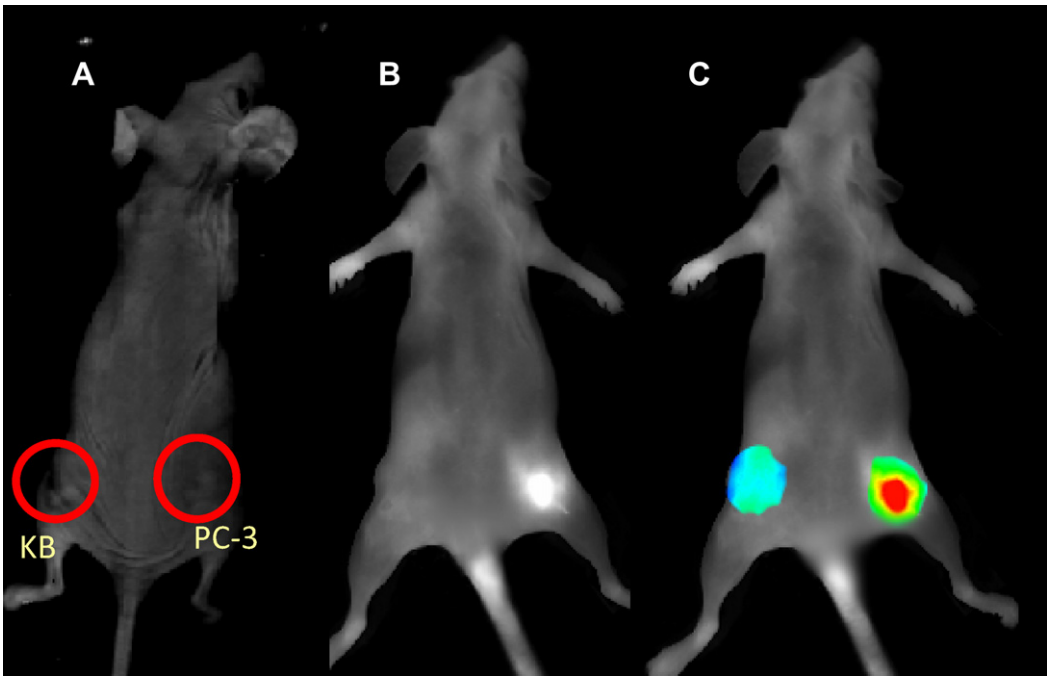

Figure 4. Mice bearing human prostate cancer xenograft (PC-3 cells) and human nasopharyngeal cancer xenograft (KB cells) were injected Gd-TTDA-NP-BN-Cy5.5 (10 nmol). Optical images showed results 0.5 h after injection. (A) White light, (B) NIR fluorescence, (C) Color mapping of B.

from the surrounding background tissue from 0.5 to 24.0 h post-injection, whereas the negative tumor could not be visualized at all time points. In addition, the quantification analysis of these images was performed. The fluorescence intensities of the tumors and the tissues as a function of time were represented in Figure 5C. The tumor uptake reached to a maximum in 0.5 h and slowly exhausted over time. Thus, we proved that the Gd-TTDA-NP-BN had high degree of specificity for GRP receptor overexpressing tumor.

2.8. Biodistribution study

To investigate the biodistribution of Gd-TTDA-NP-BN-Cy5.5 complex, the mice bearing PC-3 and KB tumors were sacrificed after optical imaging at one hour post-injection of Gd-TTDA-NP-BN-Cy5.5. Tumors and other organs were separated and subjected to optical imaging. The fluorescence images of the whole organ and tumors were obtained, as shown in Figure 6A, and % ID/g values were calculated for each organ, as illustrated in Figure 6B. The

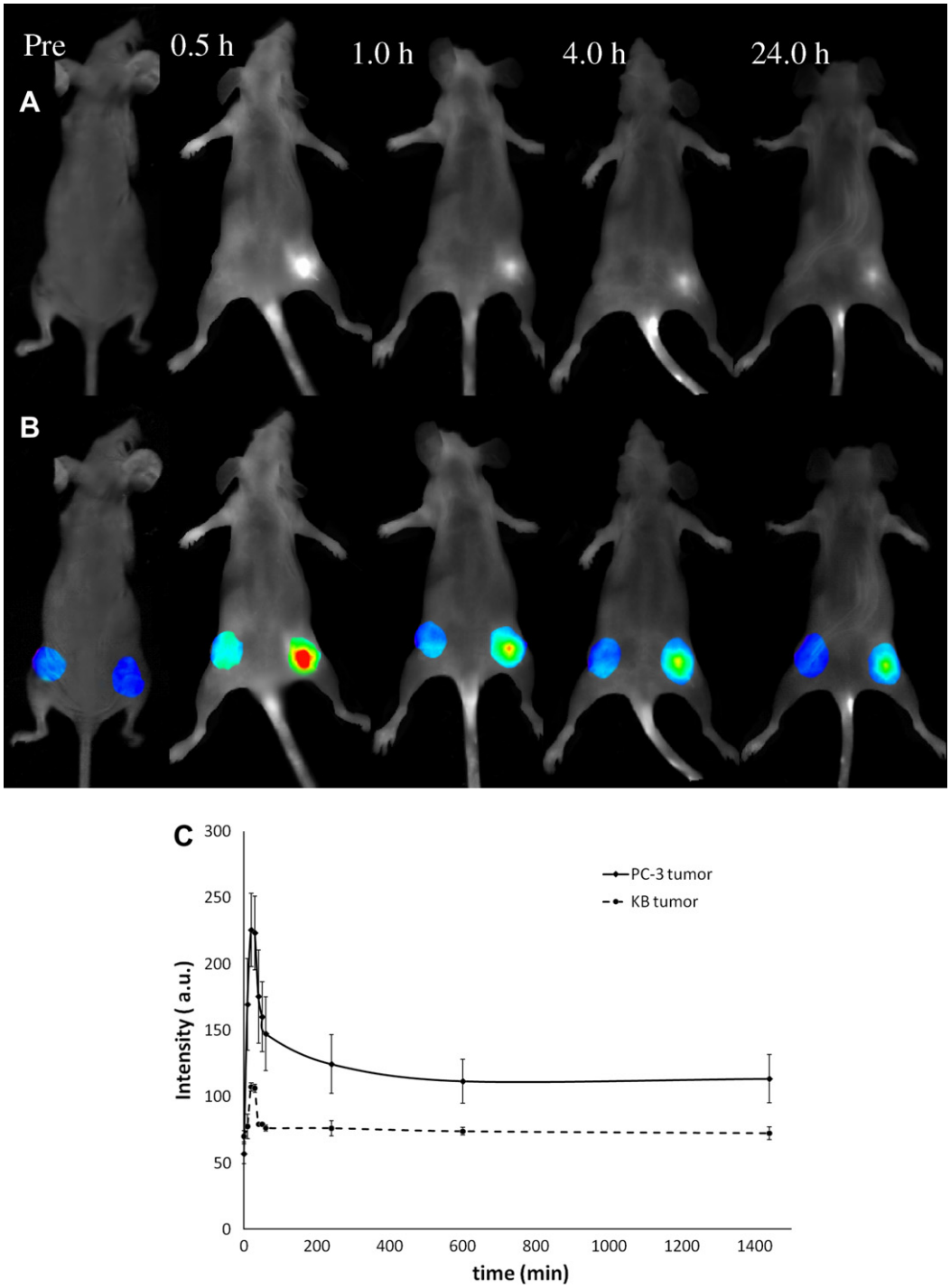

Figure 5. (A) In vivo fluorescence images of subcutaneous PC-3 and KB tumors bearing nude mice after intravenous injection of Gd-TTDA-NP-BN (10 nmol). Images were acquired at 0.5, 1.0, 4.0, and 24 h post-injection. (B) Color mapping of A, (C) Fluorescence intensity in the region of the tumor as a function of time with Gd-TTDA-NP-BN-Cy5.5.

major uptake of Gd-TTDA-NP-BN-Cy5.5 was observed in tumor, kidney, and stomach. The biodistribution data obtained at one hour post-injection indicated that the uptake of PC-3 tumor was significantly higher than that of KB tumor. On the other hand, the bone showed minor uptake which may be the release of free Gd(III) ion from the complex. The peak percentage per dose gram (% ID/g) values for PC-3 tumor, bladder, and stomach were 25.97 ± 1.07, 16.94 ± 2.15, and 16.26 ± 1.87, respectively. Tumor-to-blood, tumor-to-muscle, tumor-to-kidney, and tumor-to-liver ratios are illustrated in Figure 6C. These results are consistent with the optical imaging. It clearly demonstrates that the Gd-TTDA-NP-BN-Cy5.5 is capable of targeting GRP receptor on the PC-3 tumor.

2.9. In vitro MR imaging

To demonstrate the potential utility of the Bombesin analogue conjugated $[Gd(TTDA\text{-}NP)(H_2O)]^{2-}$, the in vitro MR imaging studies were conducted with PC-3 and KB cells using a 3.0-T MR imaging

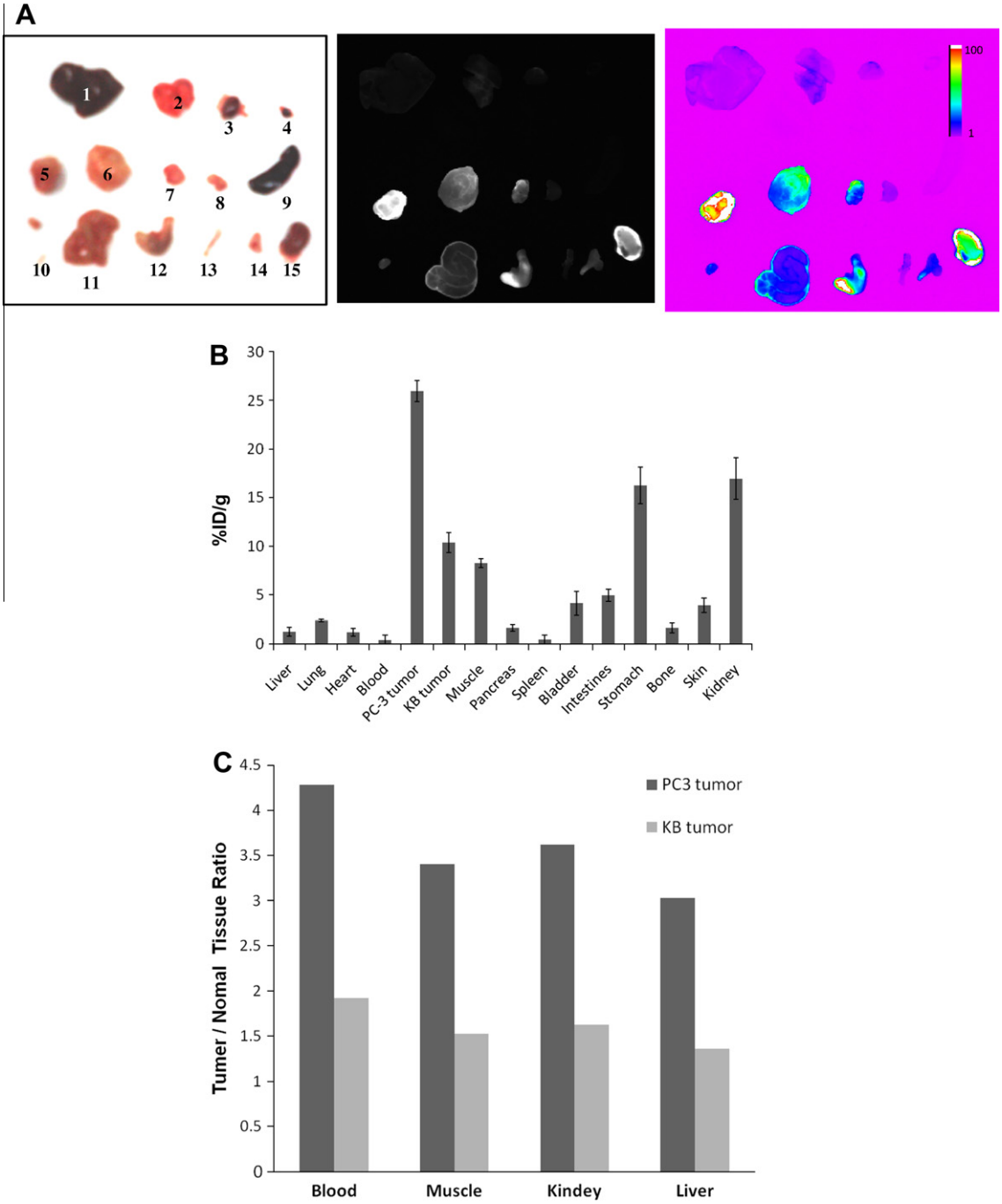

Figure 6. (A) Representative images of dissected organs of mice bearing PC-3 and KB tumors sacrificed one hour after intravenous injection of Gd-TTDA-NP-BN-Cy5.5 at a dose of 10 nmol equivalent Cy5.5/mice. (1) liver, (2) lung, (3) heart, (4) blood, (5) PC-3 tumor, (6) KB tumor, (7) muscle, (8) pancreas, (9) spleen, (10) bladder, (11) intestines, (12) stomach, (13) bone, (14) skin, and (15) kidney, (B) Biodistribution of the Gd(III) complex at one hour post-injection, (C) Tumor-to-normal tissue ratios.

scanner. Figure 7A–E showed the in vitro T_1-weighted MR images of cells without contrast agent or with $[Gd(DTPA)(H_2O)]^{2-}$, $[Gd(TTDA\text{-}NP)(H_2O)]^{2-}$, Gd-TTDA-NP-BN, and Gd-TTDA-NP-BN with fourfold excess of BN peptide, respectively. The enhancement (%) was calculated by the following (Eq. 3):

$$\text{Enhancement}(\%) = \frac{SI_{post} - SI_{pre}}{SI_{pre}} \times 100\% \quad (3)$$

where SI_{pre} is the value of signal intensity for cells untreated with the contrast agent and SI_{post} is the value of signal intensity for cells treated with the contrast agent. The signal enhancement (%) values for PC-3 cells were 2.8 ± 2.4, 32.0 ± 2.6, 68.7 ± 4.1, and 21.6 ± 2.8, respectively. The PC-3 cells showed remarkable signal enhancement comparing to KB cells, among which Gd-TTDA-NP-BN showed a maxima of 68.7% enhancement. These in vitro MR imaging results indicated that Gd-TTDA-NP-BN could efficiently target to GRP receptor overexpressing PC-3 cells. The $[Gd(DTPA)(H_2O)]^{2-}$ and $[Gd(TTDA\text{-}NP)(H_2O)]^{2-}$ did not show significant signal enhancement on the PC-3 and KB cells, because these contrast agents were not conjugated with BN peptide. In addition, the competitive study for Gd-TTDA-NP-BN with fourfold excess of BN peptide substrate was performed. Bombesin analogue peptide and Gd-TTDA-NP-BN competed on bind-

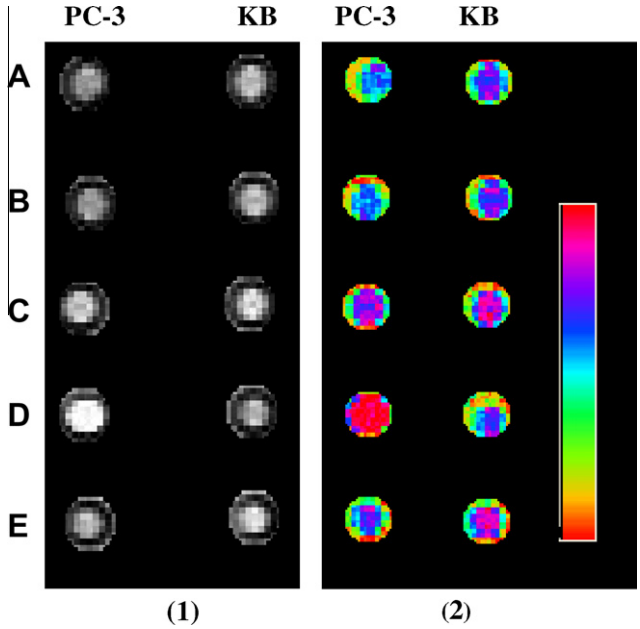

Figure 7. (1) The in vitro T_1-weighted MR images of PC-3 and KB cell after the treatment of (A) without contrast agent, (B) $[Gd(DTPA)(H_2O)]^{2-}$, (C) $[Gd(TTDA\text{-}NP)(H_2O)]^{2-}$, (D) Gd-NP-TTDA-BN, (E) Gd-TTDA-NP-BN with fourfold excess of BN, (2) Color mapping of (1).

ing to GRP receptor, and the signal enhancement was drastically reduced because of only small amount of Gd-TTDA-NP-BN uptake by PC-3 cells. These results showed that Gd-TTDA-NP-BN had significant high signal enhancement over other non-BN conjugated Gd(III) complexes.

2.10. In vivo MR imaging

The in vivo targeting ability of Gd-TTDA-NP-BN complex was examined with the mice bearing PC-3 and KB tumors. The mice bearing tumors ($n = 5$) were prepared by subcutaneous injection of the PC-3 and KB cells into the left and right lateral thighs, respectively. The MR imaging on mice was studied at predetermined time intervals after the intravenous injection of Gd-TTDA-NP-BN, and the T_1-weighted images were performed over 0.4–24 h. Figure 8 shows the comparison of the T_1-weighted fast spin-echo images of mice bearing tumor of pre- (Fig. 8 top) and post- (Fig. 8 bottom) intravenous injection of Gd-TTDA-NP-BN, $[Gd(TTDA\text{-}NP)(H_2O)]^{2-}$, and Gd-TTDA-NP-BN with fourfold excess of BN peptide, respectively. The enhancement (%) was calculated by the following (Eq. 4):

$$\text{Enhancement}(\%) = \frac{(SI_{post}/SI_{p.post}) - (SI_{pre} - SI_{p.pre})}{(SI_{pre}/SI_{p.pre})} \times 100\% \qquad (4)$$

where SI_{post} is the signal intensity after injection, $SI_{p.post}$ is the signal intensity of the phantom after injection, SI_{pre} is the signal intensity before injection, and $SI_{p.pre}$ is the signal intensity of the phantom before injection. The region-of-interest analysis over the PC-3 and KB tumors at 24 min post-injection of Gd-TTDA-NP-BN indicated that the signal enhancement percentages were 44.9 ± 4.2 and 10.45 ± 1.8, respectively. These results showed a significant signal enhancement on the PC-3 tumors. However, no remarkable signal enhancement changes on the KB tumors were observed. The Gd-TTDA-NP-BN with fourfold excess of BN had shown significant lower signal enhancement than that of Gd-TTDA-NP-BN. Conversely, no notable signal enhancement change for $[Gd(TTDA\text{-}NP)(H_2O)]^{2-}$ was observed. It clearly demonstrates that Gd-TTDA-NP-BN complex has the ability to target GRP receptor on the PC-3 tumors. Furthermore, the targeting ability of Gd-TTDA-NP-BN was also proven by comparing the signal enhancement (%) of Gd-TTDA-NP-BN as a function of time with those of $[Gd(TTDA\text{-}NP)(H_2O]^{2-}$ and Gd-TTDA-NP-BN with fourfold excess of BN peptide, as shown in Figure 9A–C. These results imply that the signal enhancement of Gd-TTDA-NP-BN is steady over an hour and then starts to decrease. On the other hand, the $Gd[(TTDA\text{-}NP)(H_2O)]^{2-}$ and Gd-TTDA-NP-BN with fourfold excess of BN did not showed any changes on their signal enhancement over 24 h. Moreover, the signal enhancements (%) of in vivo MR imaging are in good agreement with in vitro MR imaging. Hence, the Gd-TTDA-NP-BN is capable of targeting the GRP receptor of the PC-3 tumor.

3. Conclusion

In summary, we successfully synthesized Bombesin analogue conjugated Gd(III) complex for molecular optical and MR imaging. A significant increase on relaxivity (r_1) for Gd-TTDA-NP-BN was

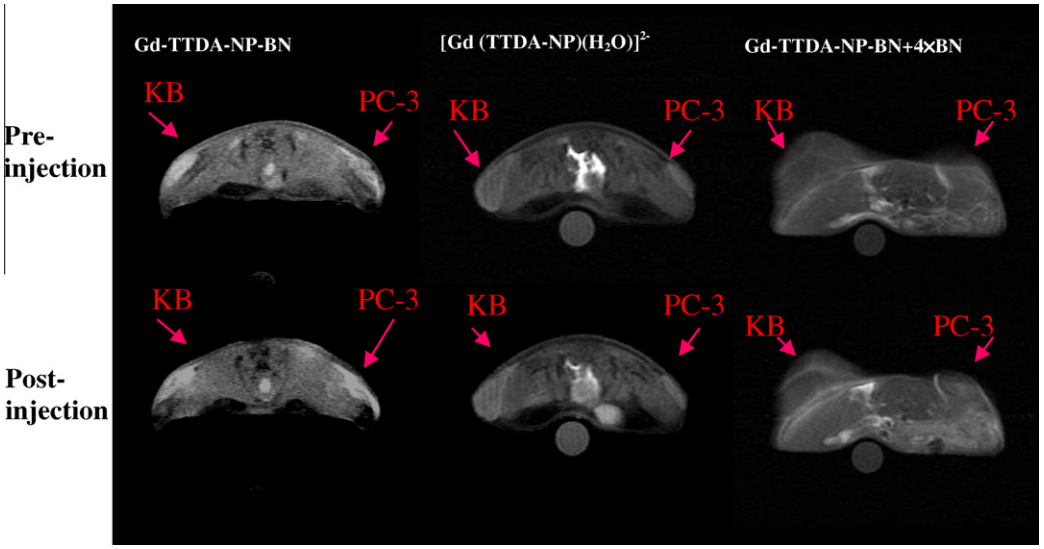

Figure 8. The in vivo T_1-weighted MR images of mice bearing PC-3 (right) and KB (left) xenografts pre- and post-injection of Gd-TTDA-NP-BN (0.1 mmol/kg), MR imaging was performed with a clinical 3.0-T MR scanner and animal coil, scanned by a Fast gradient echo pulse sequence (TR/TE/flip angel = 800/12/10°).

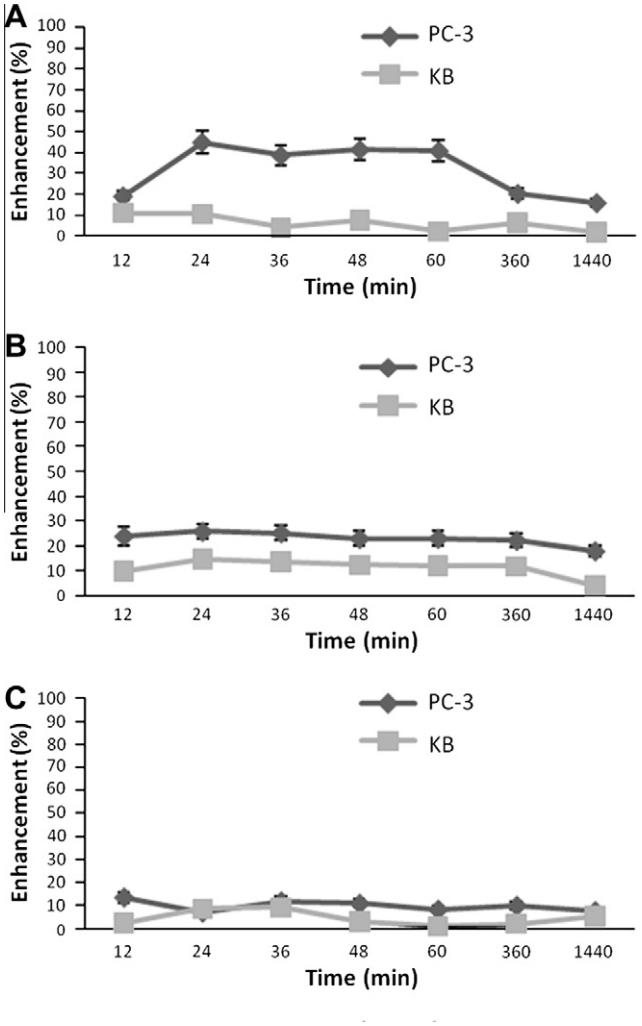

Figure 9. Plots of signal enhancements (%) of the tumor as a function of time with (A) Gd-TTDA-NP-BN, (B) Gd-TTDA-NP-BN with fourfold excess of BN, (C) $[Gd(TTDA\text{-}NP)(H_2O)]^{2-}$.

observed. The cell cytotoxicity results showed that the Gd-TTDA-NP-BN complex had low cytotoxic. Furthermore, in vitro optical imaging results reveal that this Gd(III) complex efficiently targets to PC-3 tumor cells. The biodistribution studies further showed a high level accumulation of the Gd-TTDA-NP-BN-Cy5.5 complex on the GRP receptor overexpression tumor cells. In addition, Gd-TTDA-NP-BN complex has the ability to target PC-3 tumor cells, as proven by in vitro and in vivo MR imaging studies. Thus, the Gd-TTDA-NP-BN-Cy5.5 can be potentially used as a dual contrast agent for optical/MR imaging of prostate cancer.

4. Experimental

4.1. General methods

All commercially available chemical reagents were used without further purification. Silica gel, palladium/charcoal (Pd/C), 1,2-ethanedithiol (EDT), and ninhydrin were purchased from Merck. 2-Hydroxy-5-nitrobenzyl bromide and bromoacetylbromide were purchased from Alfa aesar. Diisopropylethylamine (98%) (DIPEA), *N*-methylmorpholin 99% (NMM), triethyl silane, and hydrazine monohydrate (99%) were purchased from Acros. Trifluoroacetic acid (99%), piperidine (99.5%), pyridine, DL dithiothretiol, europium chloride, gadolinium chloride, cyanine dye (Cy5.5), 3-[4,5-dimethylthiazol-2-yl]-2,5-diphenyltetrazoplium bromide (MTT), and phosphate buffered saline were purchased from Sigma–Aldrich. 3,6,10-Triazadodecane-3,10-tetraacetic acid (tetra)-*tert*-butyl ester (TTDA-4est) (**1**) was prepared using a previously published method.[28,43] *tert*-Butylbromoacetate was synthesized according to the reported procedure.[44] Fluorescence and luminescence properties were measured using Varian Cary Eclipse fluorescence spectrophotometer and ^1H (400 MHz), ^{13}C (100 MHz), and ^{17}O (54.2 MHz) NMR spectra were recorded on a Varian Gemini-400 spectrometer. The HPLC experiments were performed on an Amersham ÄKTAbasic 10 instrument equipped with an Amersham UV-900 detector and Amersham Frac-920 fraction collector. Supelco RP-C18 column (5 μm, 4.6 × 250 mm and 5 μm, 10 × 250 mm) was used. LC-mass spectral analyses were performed with Waters Micromass-ZQ, mass spectrometry. The concentration of Gd(III) complex was determined by ICP-MS with a Perkin–Elmer OPTIMA 2000.

4.2. Synthesis

4.2.1. Synthesis of TTDA-NP (2)

TTDA-4-est (**1**) (11.19 g, 19.5 mmol) and K_2CO_3 (5.39 g, 39.0 mmol) were suspended in anhydrous CH_3CN(100 mL) and stirred for 20 min. Then the reaction mixture was treated with 2-hydroxy-5-nitrobenzyl bromide (5.72 g, 23.4 mmol) and refluxed at 80 °C for 24 h under nitrogen atmosphere. The reaction was cooled to room temperature and then the salt was filtered. The filtrate was concentrated under the reduced pressure. The resulting product was purified by silica gel column chromatography (hexane/ethyl acetate = 3:1), to give TTDA-NP-NO_2 (11.78 g, 69.2%). MS(ESI): *m/z* calad: 725.88, found: 725.65 $[M+H]^+$. ^1H NMR (400 MHz, $CDCl_3$): δ 1.43 (m, 36H, –C–(CH_3)$_3$), 1.80 (b, 2H, –CH_2–), 2.72 (q, 4H, –CH_2–), 3.00 (t, J = 6.0 Hz, 4H, –CH_2–), 3.38 (s, 8H, –CH_2–), 4.04 (b, 2H, –CH_2–), 8.00 (s, 1H, Ar-*H*), 8.10 (dd, 2H, Ar-*H*).

Subsequently, the Pd/C (240 mg) was added to the stirring solution of TTDA-NP-4 ester (9.03 g, 12.4 mmol) in CH_3CN (50 mL) under 1.5 atm H_2. This step was repeated until the pressure decreasing was stopped. Then the solvent was removed under reduced pressure. The product was purified by column chromatography (SiO_2, dichloromethane/methanol = 19:1), to give **2** (TTDA-NP-NH_2) (7.67 g, 88.7%). ^1H NMR (400 MHz, $CDCl_3$): δ 1.44 (m, 36H,–C(CH_3)$_3$), 1.74 (m, 2H,–CH_2–), 2.68 (q, 4H,–CH_2–), 2.94 (t, J = 6.5 Hz, 4H,–CH_2–), 3.37 (s, 8H,–CH_2–), 3.86 (b, 2H,–CH_2–), 6.40 (s, 1H, Ar-*H*), 6.54 (d, 2H, Ar-*H*).^{13}C NMR (100 MHz, $CDCl_3$): δ 170.6, 170.5, 168.9, 166.4, 150.4, 138.4, 116.5, 81.6, 81.2, 81.0, 56.0, 55.8, 55.7, 51.9, 51.5, 51.4, 28.1.

4.2.2. Synthesis of TTDA-NP-NCS (3)

TTDA-NP-NH_2 (2) (5.36 g, 7.87 mmol) was dissolved in THF (40 mL) and the resulting reaction mixture was cooled in an ice bath and then thiophosgene (1.9 mL, 25.97 mmol) was slowly added under nitrogen atmosphere. The stirring was continued for 3 h and then the solvent was removed under the reduced pressure. Purification by chromatography (silica, dichloromethane/methanol = 19:1), produces a yellow oil substance **3** (2.24 g, 38.7%). ^1H NMR (400 MHz, $CDCl_3$): δ 1.45 (m, 36H,–C–(CH_3)$_3$), 1.92 (b, 2H,–CH_2–), 2.79 (b, 4H,–CH_2–), 3.00 (b, 4H,–CH_2–), 3.36 (s, 8H,–CH_2–), 3.87 (b, 2H,–CH_2–), 7.03 (s, 1H, Ar-*H*), 7.11 (d, 2H, Ar-*H*).^{13}C NMR (100 MHz, $CDCl_3$): δ 170.5, 170.4, 157.4, 126.5, 122.7, 121.6, 117.4, 81.3, 81.1, 56.0, 55.8, 55.7, 51.8, 51.2, 47.5, 28.1.

4.2.3. Synthesis of peptide

The solid-phase peptide synthesis was performed on a Rink Amide resin (0.63 mmol/g loading) by using the Fmoc chemistry. They were assembled on a PS-3 (Automated Peptide Synthesizer). The side chain protecting groups of trifunctional amino acids were trifluoroacetic acid labile. BN peptide (Bombesin analogue) was

synthesized on a 0.128 mmol scale using a fourfold molar excess of Fmoc-protected amino acids (0.512 mmol), which were activated by using fourfold excess of bromo-tris-pyrrolidino phosphonium hexafluorophosphate (PyBoP) in the presence of *N*-methylmorpholin (NMM) (20% v/v) in dimethylformamide. N^{α}-Fmoc protecting groups were removed by treating the resin-attached peptide with piperidine (20% v/v) in dimethylformamide. The Bombesin analogue functionalized resin (0.5 g, 0.63 mmol/g, 0.31 mmol) was deprotected with the piperidine solution and was washed with the dimethylformamide as described above.

4.2.4. Conjugation of ligand to peptide substrate (4)

In a separate vial, TTDA-NP-NCS (0.914 g, 1.24 mmol) and diisopropylethylamine (0.16 g, 1.24 mmol) were dissolved in 10 mL of dimethyl sulfoxide. The resulting solution was added to the deprotected resin, and nitrogen gas was bubbled through the mixture for 24 h. The peptide solution was removed. The resin was washed with dimethylformamide and methanol, and then was dried under vacuum. A solution of 95% trifluoroacetic acid, 2.5% 1, 2-ethanedithiol, 1.5% water, and 1.0% triethyl silane (10 mL) were added to the resin, and the nitrogen was bubbled through the mixture for 2 h. Then the cleaved peptide was precipitated in ice-cold diethyl ether and centrifuged at 1500 rpm for 5 min. Purification was performed by preparative HPLC using a C18 column. Elution was performed with a solvent system consisting of 0.1% CF_3COOH/H_2O (solvent B) and CF_3COOH/CH_3CN (solvent A), by applying the following gradient: from 95% solvent B to 40% solvent A over 100 min at flow rate of 1 mL/min (retention time: 17.5 min by UV detector at 256, 280 nm). The collected fractions were combined and lyophilized to yield the product **4** as a pink powder (229.6 mg, 42.3%). MS (ESI): *m/z* calcd: 1751.98, found: 1751.20 $[M+H]^+$.

4.2.5. Synthesis of Gd-TTDA-NP-BN (6)

TTDA-NP-BN (100 mg, 0.057 mmol) was dissolved in deionized water (8 mL) and pH 6.0–7.0 was adjusted by slowly adding sodium hydroxide. Then 340 μL of $GdCl_3$ (161.25 mM) was added and the mixture was stirred for 48 h at 37 °C. The completion of complex formation was confirmed by xylenol orange test. The solution was filtered and the filtrate was lypophilized. A white powder product **6** was obtained. The purity of Gd-TTDA-NP-BN was determined by HPLC and the identity was confirmed by mass. MS (ESI): *m/z* calcd: 1904.19, found: 1908.60 $[M+4H]^+$.

4.2.6. Synthesis of Eu-TTDA-NP-BN (7)

TTDA-NP-BN (20 mg, 0.014 mmol) was dissolved in deionized water (3 mL) and pH 6.0–7.0 was adjusted by slowly adding sodium hydroxide. The resulting solution was stirred for 10 min, followed by the addition of 72.4 μL of $EuCl_3$ (161.25 mM). The stirring was continued for 48 h at 37 °C. Subsequently, the solution was filtered and the filtrate was lyophilized to give **7**. The purity of Gd-TTDA-NP-BN was analyzed by HPLC and identified by mass. MS (ESI): *m/z* calcd: 1998. 91, found: 1999.40 $[M+H]^+$.

4.2.7. Synthesis of Gd-TTDA-NP-BN-Cy5.5 (8)

Gd-TTDA-NP-BN (2.42 mg, 1.47 μmol) was dissolved in 0.1 M sodium borate ($Na_2B_4O_7$) at pH 8.3 and then NHS-Cy5.5 (2 mg, 1.78 mL) was added. The resulting reaction mixture was stirred in dark, at room temperature for 12 h and purified by preparative HPLC. The collected fractions were combined and lyophilized to afford **8**, (3.5 mg, 75.1%). MS(ESI): *m/z* calcd: 2800.11, found: 2801.50 $[M+H]^+$.

4.3. Relaxation time measurement

Relaxation times T_1 of aqueous solutions of Gd(III) complex were measured to determine relaxivity r_1. All measurements were made using a 20 MHz relaxometer operating at 37.0 ± 0.1 °C (NMS-120 Minispec, Bruker). Before each measurement, the relaxometer was tuned and calibrated. The values of r_1 were determined from six data points generated by an inversion-recovery pulse sequence. The proton spin-lattice relaxation (T_1) was measured by using various concentrations of Gd(III) complexes at 37.0 ± 0.1 °C in PBS buffer (pH 7.4).

4.4. Luminescence method for establishing solution hydration state

Luminescence lifetime data has been obtained for the Eu(III) complex to determine the number of inner-sphere water molecules in the aqueous solution.[39–41] The luminescence lifetime (τ) has been determined in both H_2O and D_2O. The complex containing the number of inner-sphere water was calculated by (Eqs. 1 and 2). The *q* value is obtained from the luminescence study.

4.5. Variable-temperature ^{17}O NMR measurement

The measurement of the ^{17}O transverse relaxation rates, longitudinal relaxation rates, and chemical shifts was carried out with a Varian Gemini-400 spectrometer, equipped with a 10 mm probe, by using an external D_2O lock. The Varian 600 temperature control unit was used to stabilize the temperature in the range 278–338 K. Solutions containing 5.5% of the ^{17}O isotope were used. The inversion-recovery of method was applied to measure longitudinal relaxation rates, $1/T_1$, and the Carr-Purcell-Meiboom-Gill spin-echo technique was used to obtain transverse relaxation rates, $1/T_2$. The solution was introduced into spherical glass containers, fitting into ordinary 10 mm NMR tubes, in order to eliminate magnetic susceptibility corrections to chemical shifts.

4.6. Cell culture and animal model

PC-3 cell is a human prostate cancer cell line overexpressing gastrin releasing peptide (GRP) receptors.[45] KB cell is a human nasopharyngeal epidermal carcinoma cell line, lacking of the expression of GRP receptors. All cells were obtained from American Type Culture Collection (Manassas, VA). PC-3 and KB cells were cultured in RPMI 1640 medium (GIBCO) and Ham's F12 K medium (GIBCO), respectively. All media were supplemented with 10% of fetal bovine serum, sodium bicarbonate (1.5 g/L), sodium pyruvate (1.0 mM), and non-essential amino acid (0.1 mM). Cells were cultured at 37 °C in a humidified 5% CO_2 atmosphere. BALB/cAnN.Cg-Foxn1^{nu}/CrlNarl mice (5 weeks old, male) were purchased from the National Laboratory Animal Center, Taipei, Taiwan. Animal experiments were performed in accordance with the institutional guidelines. PC-3 and KB cells in 100 μL (10^6 cells) PBS were subcutaneously injected into five nude mice. The cells were mixed in equal volume with Matrigel and injected into the right (PC-3) and left (KB) lateral thighs of the mice. An MR imaging experiment was performed 2 weeks after the tumor implantation, at which time the tumors were measured to be at least 100 mm^3. This method produces a high yield of tumor in the lateral thighs of nude mice.

4.7. Cell cytotoxicity

PC-3 and KB cell lines were used to measure the in vitro cell cytotoxicity of Gd-TTDA-NP-BN. An amount of 10^5 cells was plated in each well of the 96-well plates for 24 h. Then, the Gd-TTDA-NP-BN were added at the desired concentrations (from 0.125 to 2.0 mM Gd(III) complex per well). After 24 h of incubation, the supernatant was removed and the cells were washed three times with PBS. Cell viability was estimated using the 3-(4,5-dimethyl-

thiazol-2-yl)-2,5-diphenyltetrazolium bromide (MTT) conversion test. Briefly, MTT (50 μL) solution was added to each well. After 2 h of incubation, each well was treated with dimethyl sulfoxide (50 μL) with pipetting. Absorption at 570 nm was measured on ELISA reader. The data represent the average of sixteen wells. The viability of untreated cells was assumed to be 100%.

4.8. In vitro specific targeting study of Eu-NP-TTDA-BN

The specific targeting study was investigated by using Eu-TTDA-NP-BN complex. PC-3 cell lines were used to measure the in vitro specific targeting study. About 10^5 cells were plated in each well of the 6-well plates for 24 h. Then, Eu-TTDA-NP-BN was added at the predetermined concentrations (1 mM, Eu-TTDA-NP-BN per well) and incubated at 4.0 and 37.0 °C. After one hour the supernatant was removed and the cells were washed three times with PBS buffer. Then, the cells were treated with paraformaldehyde (4%, 0.5 mL) solution for 10 min to fix the cells, and washed with PBS buffer. Finally, the cells were inspected using a confocal fluorescence microscopy (exciter, 360/30 nm; emitter, 400/20 nm).

4.9. In vitro optical imaging of Gd-TTDA-NP-BN-Cy5.5

PC-3 and KB cell lines were also used to measure the in vitro specific targeting of Gd-TTDA-NP-BN-Cy5.5. About 10^5 cells were plated in each well of the 24-well plates for 24 h. Then, Gd-TTDA-NP-BN-Cy5.5 was added at the predetermined concentrations (10 μM per well). After one hour of incubation at 37 °C, the supernatant was removed and the cells were washed three times with PBS. In addition, the nucleus was stained with 4′,6-diamidino-2-phenylindole (200 nM) solution for 3 min, followed by washing with PBS buffer three times, and the cells were inspected using fluorescence microscopy, a ZEISS Axio imager M1 microscope stand with TFT monitor equipped with DAPI filters (exciter, 360/30 nm; emitter, 400/20 nm) and Cy5.5 filters (exciter, 650/20 nm; emitter, 675/35 nm) to observe the cellular localization.

4.10. In vivo optical imaging

In vivo fluorescence imaging was performed using Kodak image station 2000 MM digital imaging system from molecular imaging systems, Carestream Health, Inc. For the optical imaging experiment, mice ($n = 5$) were injected via tail vein with 10 nmol of Gd-TTDA-NP-BN-Cy5.5 and subjected to optical imaging at various time points of post-injection. All NIR fluorescence images were acquired using 10 s exposure times.

4.11. Biodistribution study

Gd-TTDA-NP-BN-Cy5.5 (10 nmol) was intravenously injected into male nude mice. The mice ($n = 5$) were sacrificed one hour after the intravenous injection of Gd-TTDA-NB-BN-Cy5.5. Blood, lung, liver, spleen, heart, muscle, pancreas, bladder, intestines, kidney, stomach, bone, skin, PC-3, and KB tumors were collected and washed with 10 mL of PBS buffer. The fluorescence of whole organs was measured by Kodak image station 2000 MM, digital imaging system from molecular imaging systems, Carestream Health, Inc. The results were calculated as a percentage of injected dose per gram of tissue (% ID/g).

4.12. In vitro MR imaging

MR imaging studies were performed with a clinical 3.0-T magnetic resonance scanner (Sigma; GE Medical Systems, Milwaukee, WI, USA) and a knee coil. All cell lines contained 2×10^6 cells and were incubated with Gd-TTDA-NP-BN, $[Gd(TTDA\text{-}NP)(H_2O)]^{2-}$, and $[Gd(DTPA)(H_2O)]^{2-}$, (diluted in 1 mL medium, 1 mM Gd) at 37.0 ± 0.1 °C for 30 min, and then washed three times with PBS buffer. Competitive targeting of free BN peptide to Gd-TTDA-NP-BN was also studied with co-incubates of Gd-TTDA-NP-BN and fourfold excess of free BN peptide. All samples were scanned by a fast gradient echo pulse sequence (TR/TE/flip angle = 100/5.8/10°).

4.13. In vivo MR imaging

Nude mice bearing PC-3 and KB tumors were studied by MR imaging when the subcutaneous tumor xenografts reached a volume of 100 mm^3. A solution of Gd-TTDA-NP-BN (0.1 mmol/kg) was injected via the tail vein. The MR imaging of pentobarbital-anesthetized mice were performed at 0, 1, 6, and 24 h respectively, using a 3.0-T magnetic resonance scanner and a high-resolution animal coil (3.8 cm diameter, GE homemade). All animals were scanned using a T_1-weighted fast spin-echo sequence (TR/TE/flip angle = 100/5.8/10°) for imaging.

Acknowledgment

Funding from National Science Council of Taiwan (Grant Nos. NSC 98-2627-M-009-009, NSC 97-2113-M-009-016-MY3, and NSC 97-2623-7-037-001-NU) is gratefully acknowledged.

Supplementary data

Supplementary data associated with this article can be found, in the online version, at doi:10.1016/j.bmc.2010.04.040.

References and notes

1. Bogdanov, A. J.; Matuszewski, L.; Bremer, C.; Petrovsky, A.; Weissleder, R. *Mol. Imaging* **2002**, *1*, 16.
2. Su, Z.-F.; Liu, G.; Gupta, S.; Zhu, Z.; Rusckowski, M.; Hnatowich, D. J. *Bioconjugate Chem.* **2002**, *13*, 561.
3. Haubner, R.; Kuhnast, B.; Mang, C.; Weber, W. A.; Kessler, H.; Wester, H. J.; Schwaiger, M. *Bioconjugate Chem.* **2004**, *15*, 61.
4. Dijkgraaf, I.; Kruijtzer, J. A. W.; Frielink, C.; Soede, A. C.; Hilbers, H. W.; Oyen, W. J. G.; Corstens, F. H. M.; Liskamp, R. M. J.; Boerman, O. C. *Nucl. Med. Biol.* **2006**, *33*, 953.
5. Juran, S.; Walther, M.; Stephan, H.; Bergamann, R.; Stainbach, J.; Kraus, W.; Emmerling, F.; Comba, P. *Bioconjugate Chem.* **2009**, *20*, 347.
6. Liu, Z.; Yan, Y.; Liu, S.; Wang, F.; Chen, X. *Bioconjugate Chem.* **2009**, *20*, 1016.
7. Zhang, H.; Schuhmacher, J.; Waser, B.; Wild, D.; Eisenhut, M.; Reubi, J. C.; Maecke, H. R. *Eur. J. Nucl. Med. Mol. Imaging* **2007**, *34*, 1198.
8. Liu, Z.; Li, Z.-B.; Cao, Q.; Liu, S.; Wang, F.; Chen, X. *J. Nucl. Med.* **2009**, *50*, 1168.
9. Weissleder, R.; Mahmood, U. *Radiology* **2001**, *219*, 316.
10. Caravan, P.; Ellison, J. J.; McMurry, T. J.; Lauffer, R. B. *Chem. Rev.* **1999**, *99*, 2293.
11. Caravan, P. *Chem. Soc. Rev.* **2006**, *35*, 512.
12. Aime, S.; Cabella, C.; Colombatto, S.; Crich, S. G.; Gianolio, E.; Maggioni, F. *J. Magn. Reson. Imaging* **2002**, *16*, 394.
13. De Leon-Rodriguez, L. M.; Kovac, Z. *Bioconjugate Chem.* **2008**, *19*, 391.
14. Hsu, A. R.; Hou, L. C.; Veeravagu, A.; Greve, J. M.; Vogel, H.; Tse, V.; Chen, X. *Cancer Res.* **2004**, *64*, 8009.
15. Kim, S.; Lim, Y. T.; Soltesz, E. G.; De Grand, A. M.; Lee, J.; Nakayama, A.; Parker, J. A.; Mihaljevic, T.; Laurence, R. G.; Dor, D. M.; Cohn, L. H.; Bawendi, M. G.; Frangioni, J. V. *Nat. Biotechnol.* **2004**, *22*, 93.
16. Weissleder, R.; Tung, C. H.; Mahmood, U.; Bogdanov, A., Jr. *Nat. Biotechnol.* **1999**, *17*, 375.
17. Ke, S.; Wen, X.; Gurfinkel, M.; Charnsangavej, C.; Wallace, S.; Sevick-Muraca, E. M.; Li, C. *Cancer Res.* **2003**, *63*, 7870.
18. Anastasi, A.; Erspamer, V.; Bucci, M. *Arch. Biochem. Biophys.* **1972**, *148*, 443.
19. Anastasi, A.; Erspamer, V.; Bucci, M. *Experientia* **1971**, *27*, 166.
20. Katsuno, A.; Pradhan, T.; Ryan, T. K.; Mantey, R. R.; Hou, S. A.; Donohue, W.; Akeson, P. J.; Spindel, E. R.; Battey, J. F.; Coy, D. H.; Jensen, R. T. *Biochemistry* **1999**, *38*, 7307.
21. Jensen, R. T.; Moody, R. T.; Pert, C.; Rivier, J. E.; Gardner, J. D. *Proc. Natl. Acad. Sci. U.S.A.* **1978**, *75*, 6139.
22. Ferris, H. A.; Carrol, R. E.; Lorimer, D. L.; Benya, R. V. *Peptides* **1997**, *18*, 663.
23. Gugger, M.; Reubi, J. C. *Am. J. Pathol.* **1999**, *155*, 2067.
24. Markwalder, R.; Reubi, J. C. *Cancer Res.* **1999**, *59*, 1152.
25. Scheffel, U.; Pomper, M. G. *J. Nucl. Med.* **2004**, *45*, 1277.
26. De Visser, M.; Verwijnen, S. M.; De Jong, M. *Cancer Biother. Radiopharm.* **2008**, *23*, 137.
27. Maina, T.; Nock, B.; Mather, S. *Cancer Imaging* **2006**, *6*, 153.

28. Wang, Y. M.; Li, C. R.; Huang, Y. C.; Ou, M. H.; Liu, G. C. *Inorg. Chem.* **2005**, *44*, 382.
29. Ou, M. H.; Tu, C. H.; Tsai, S. C.; Lee, W. T.; Liu, G. C.; Wang, Y. M. *Inorg. Chem.* **2006**, *45*, 244.
30. Laus, S.; Ruloff, R.; Toth, E.; Merbach, A. E. *Chem. Eur. J.* **2003**, *9*, 3555.
31. Jaszberenyi, Z.; Angelique, S.; Toth, E.; Benmelouka, M.; Merbach, A. E. *Dalton Trans.* **2005**, 2713.
32. Torres, S.; Martins, J. A.; Andre, J. P.; Pereira, G. A.; Kiraly, R.; Brucher, R.; Helm, L.; Toth, E.; Geraldes, C. F. G. C. *Eur. J. Inorg. Chem.* **2007**, 5489.
33. Toth, E.; Helm, L.; Merbach, A. E. *Top. Curr. Chem.* **2002**, *221*, 61.
34. Ratnakar, S. J.; Alexander, V. *Eur. J. Inorg. Chem.* **2005**, 3918.
35. Abiraj, K.; Jaccard, H.; Kretzschmar, M.; Helm, L.; Maecke, H. R. *Chem. Commun.* **2008**, 3248.
36. Micskei, K.; Powell, D. H.; Helm, L.; Brucher, E.; Merbach, A. E. *Magn. Reson. Chem.* **1993**, *31*, 1011.
37. Wang, Y. M.; Lee, C. H.; Liu, G. C.; Sheu, R. S. *J. Chem. Soc., Dalton Trans.* **1998**, 4113.
38. Micskei, K.; Helm, L.; Brucher, E.; Merbach, A. E. *Inorg. Chem.* **1993**, *32*, 3844.
39. Horrocks, W. D.; Sudnick, D. R., Jr. *J. Am. Chem. Soc.* **1979**, *101*, 334.
40. Horrocks, W. D.; Sudnick, D. R., Jr. *Acc. Chem. Res.* **1981**, *14*, 384.
41. Beeby, A.; Clarkson, I. M.; Dickins, R. S.; Faulkner, S.; Parker, D.; Royle, L.; Sousa, A. S. D.; Williams, J. A. G.; Woods, M. *J. Chem. Soc., Perkin Trans. 2* **1999**, 493.
42. Aime, S.; Botta, M.; Fasano, M.; Crich, S. G.; Terreno, E. *J. Biol. Inorg. Chem.* **1996**, *1*, 312.
43. Grassman, W.; Wunsch, E.; Deufel, P.; Zwick, A. *Chem. Ber.* **1958**, *91*, 538.
44. Vollmar, A.; Dunn, M. S. *J. Org. Chem.* **1960**, *25*, 387.
45. Rogers, B. E.; Bigott, H. M.; McCarthy, D. W.; Manna, D. D.; Kim, J.; Sharp, J. L.; Welch, M. J. *Bioconjugate Chem.* **2003**, *14*, 756.